



National Aeronautics and Space Administration

Effect of Tungsten L-PBF Feedstock Modification on Performance in Bending

Eric Brizes^a

Elizabeth Young-Dohe^a

Justin Milner^a

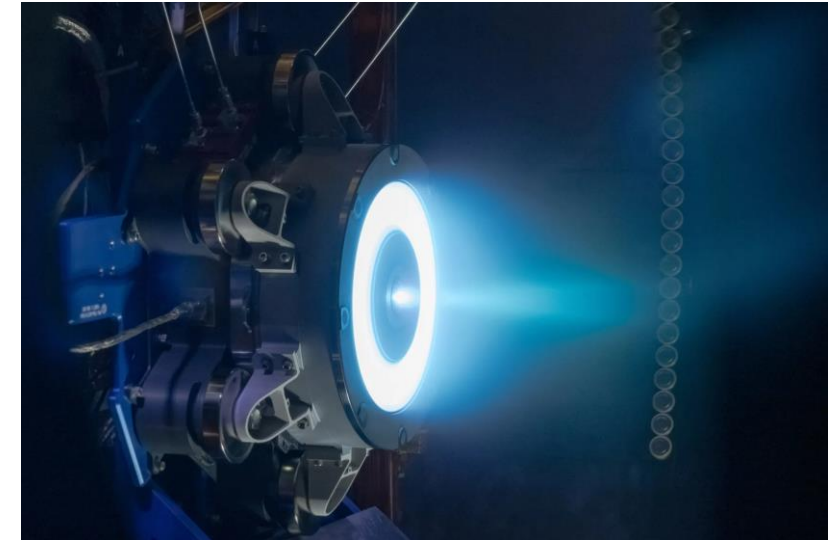
^a NASA Glenn Research Center, Cleveland, OH

TMS 2024. Orlando, FL. March 3-7



Introduction

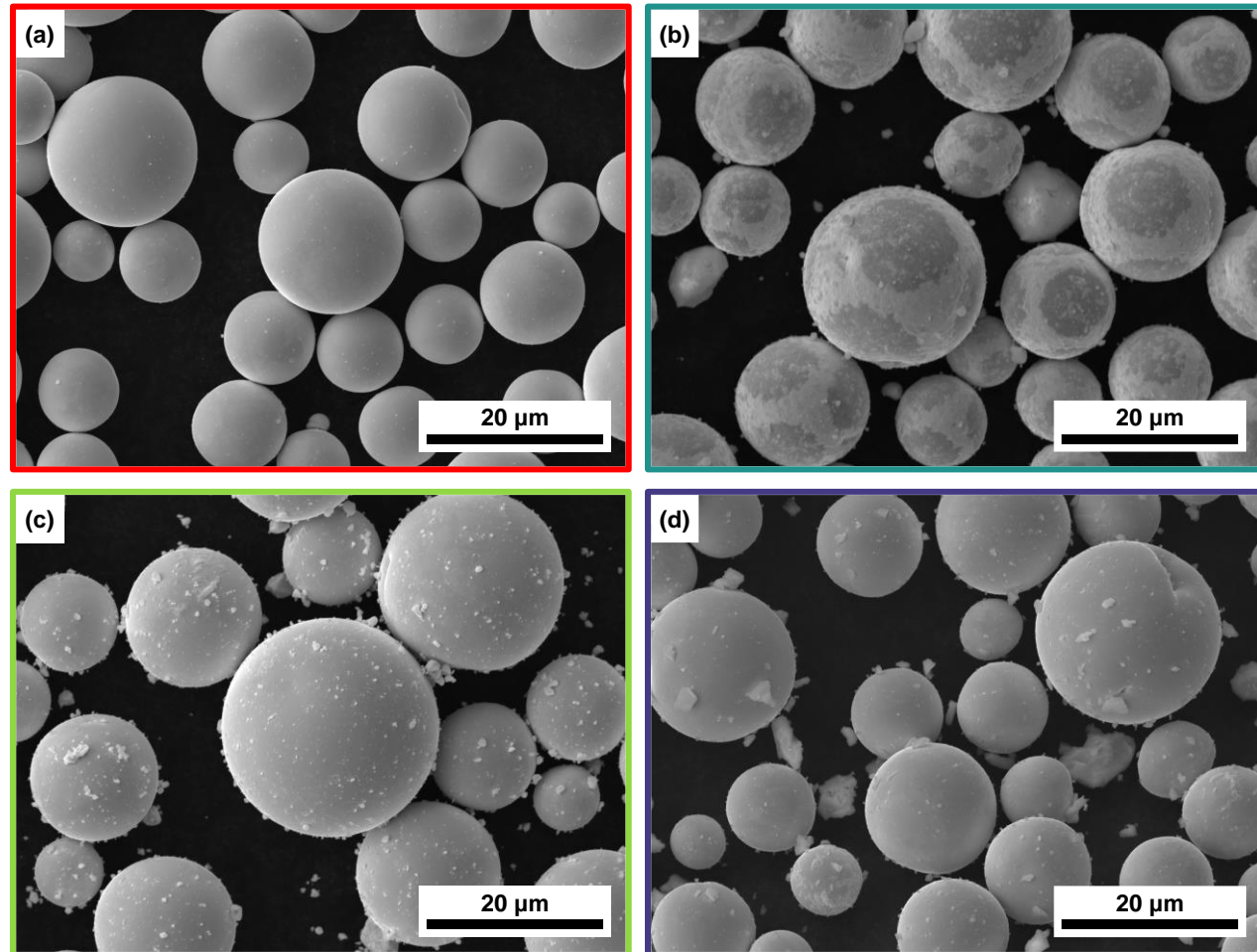
- Additively manufactured tungsten is a candidate material for high-temperature aerospace and nuclear fusion/fission applications.
- The printability of pure tungsten is challenged by cracking defects from the metal's high BDTT and low solubility of interstitial impurities. Micro-alloying and dispersoid additions can alter tungsten printability and strength.
- In this work, pure tungsten L-PBF feedstock was modified with 1 wt% additions of ceramic compound nano-powders. Flexural strength and microstructural characterization assessed the effect of the feedstock modification on mechanical performance.



The Advanced Electric Propulsion System (AEPS) inside a vacuum chamber at NASA Glenn Research Center. Credit: NASA / Jef Janis

Materials and Powder Processing

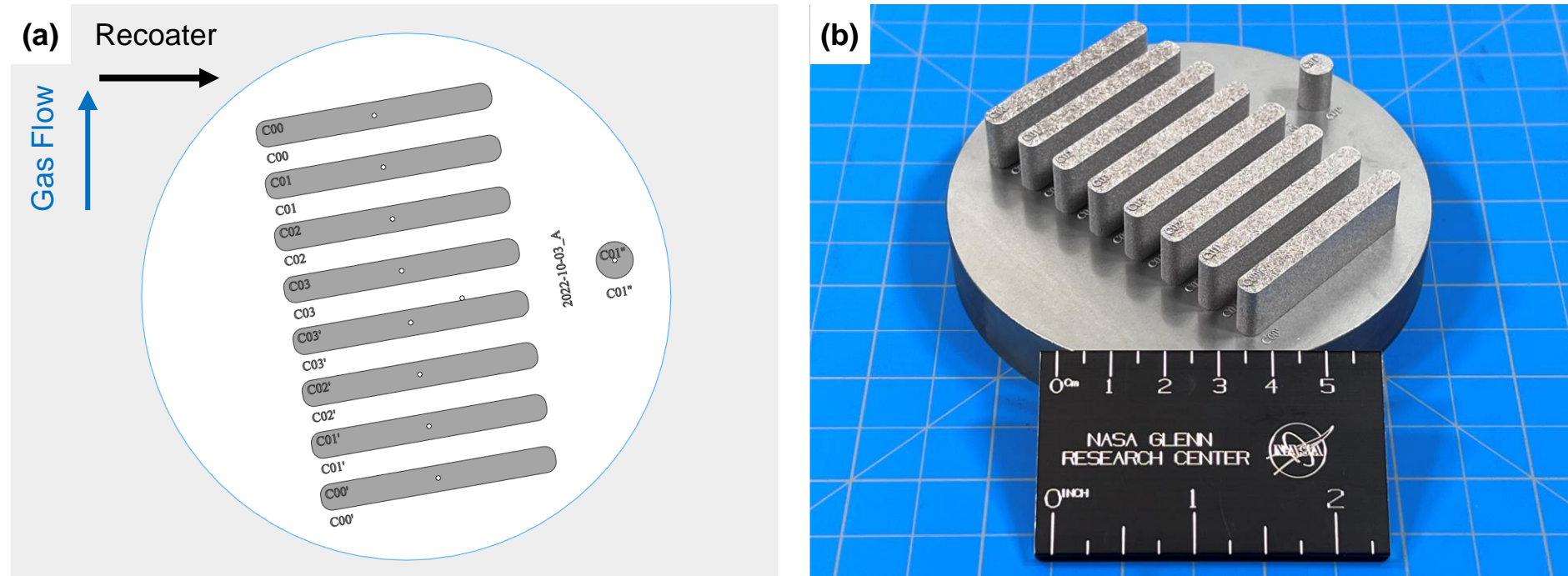
- Barstock
 - Wrought (worked)
 - Cast (electron beam)
- L-PBF Feedstock
 - **99.9% Tungsten**
 - $D_{10} = 10 \mu\text{m}$
 - $D_{90} = 25 \mu\text{m}$
- Nanoparticles
 - HfO_2 (100 - 200 nm)
 - HfC (100 - 200 nm)
 - ZrH_2 (1 - 5 μm)



SEM secondary electron images of (a) Pure tungsten, (b) Tungsten + 1 wt% HfO_2 , (c) Tungsten + 1 wt% HfC , (d) Tungsten + 1 wt% ZrH_2

Additive Manufacturing

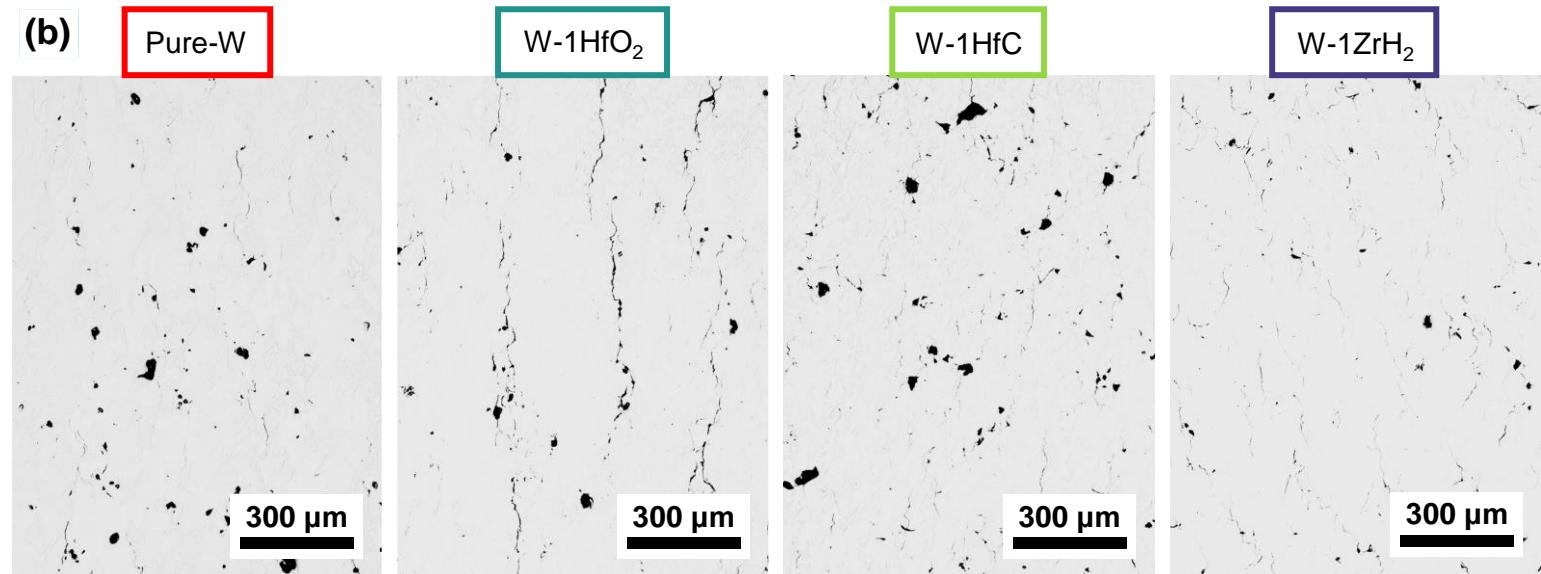
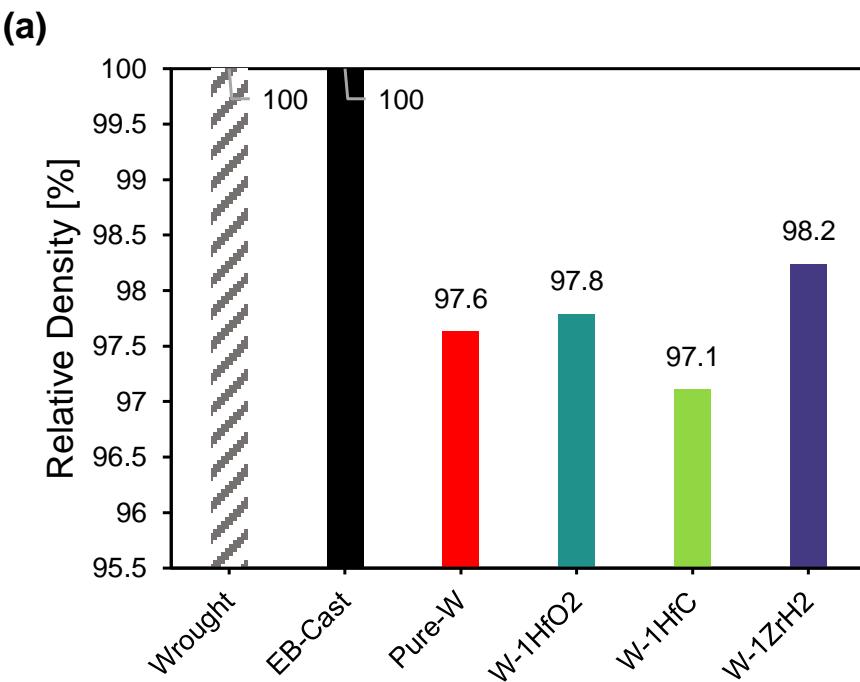
- EOS M100, 283 - 708 J/mm³, < 200 ppm O₂



(a) Layout of specimens on the build plate and (b) The as-fabricated specimens

Printed Material Relative Density

- Determined via image analysis



(a) Relative density of all examined tungsten samples, (b) Example of optical micrographs from which image analysis determined L-PBF material relative density



Printed Material Chemical Composition

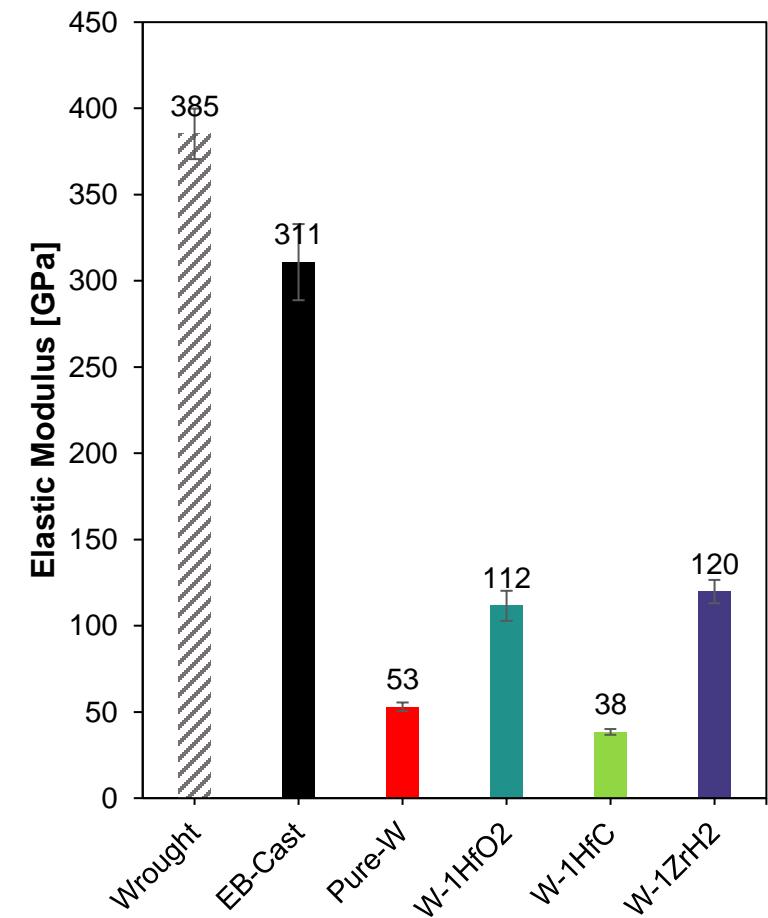
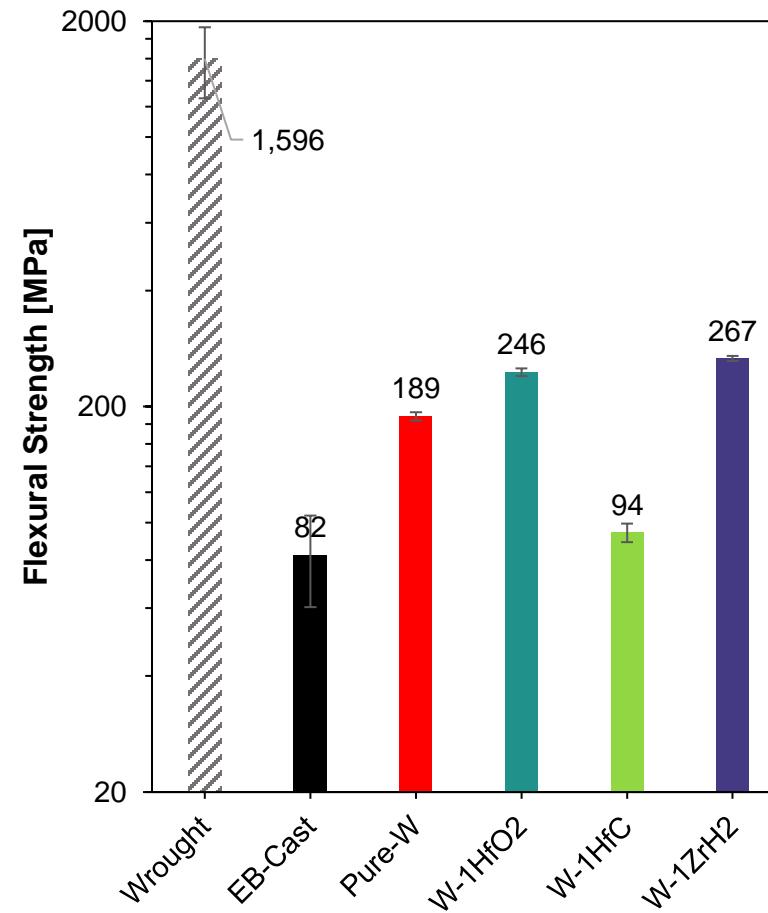
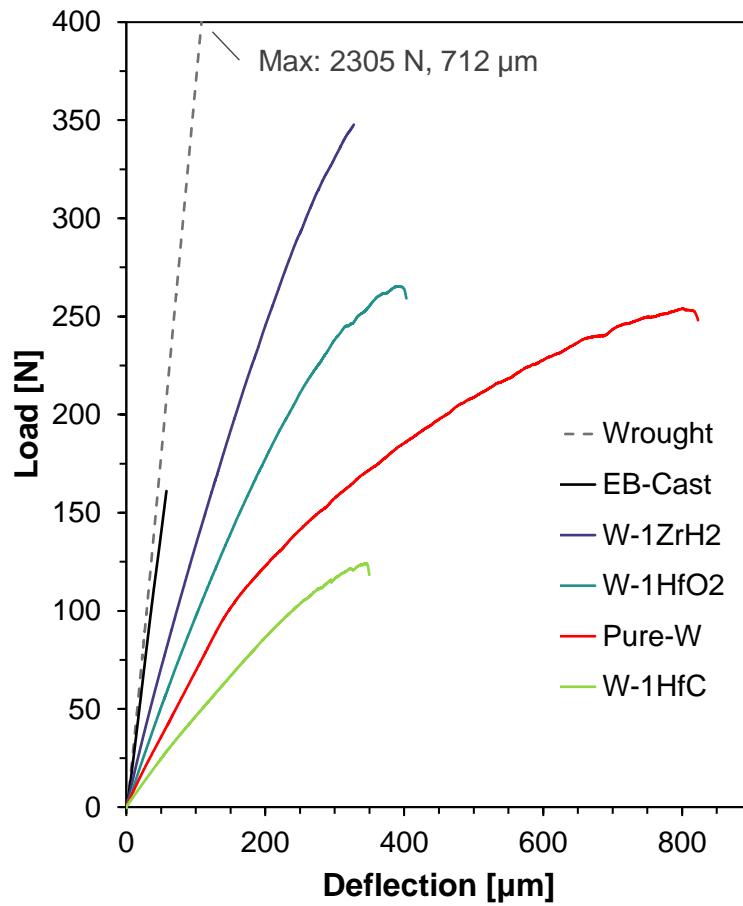
- Determined via ICP-MS and LECO Combustion analysis

| Material | W [wt%] | Hf [wt%] | Zr [wt%] | Ti [wt%] | O [ppm] | N [ppm] | C [ppm] | H [ppm] |
|---------------------|---------|----------|----------|----------|---------|---------|---------|---------|
| Pure-W | 99.9 | - | - | - | 36 | - | - | - |
| W-1HfO ₂ | 99.7 | 0.310 | - | - | 340 | - | - | 1 |
| W-1HfC | 99.1 | 0.840 | 0.010 | - | 14 | 11 | 350 | 1 |
| W-1ZrH ₂ | 99.4 | 0.015 | 0.570 | 0.002 | 88 | 17 | - | 1 |

A dash symbolizes a result of “not detected”

Four-point Bend Testing

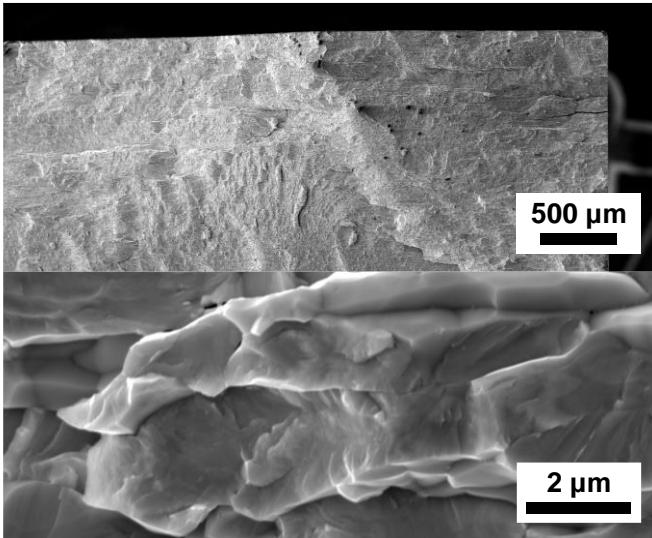
- Per ASTM C1161-18
 - Specimen Geometry: 45 x 4 x 3 mm



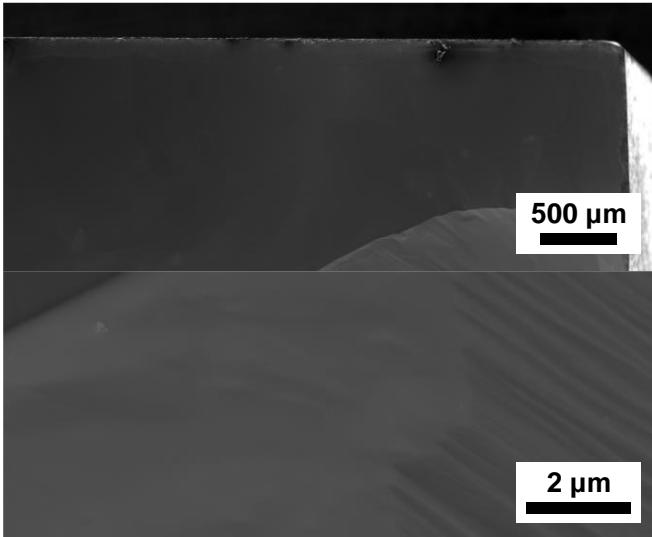
Fractography



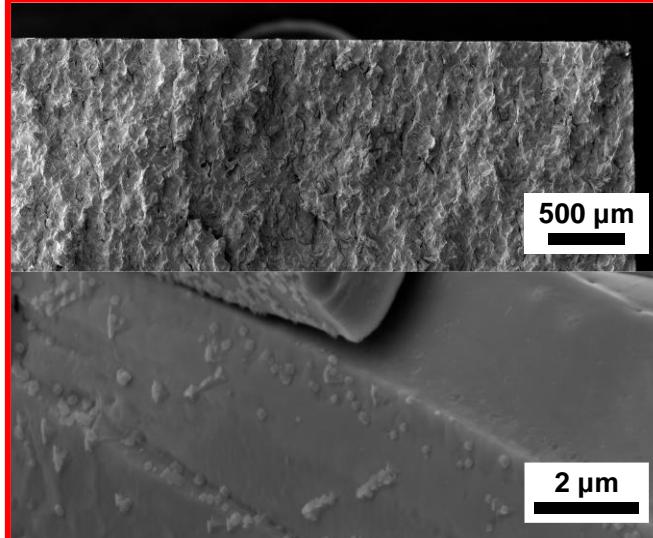
Wrought



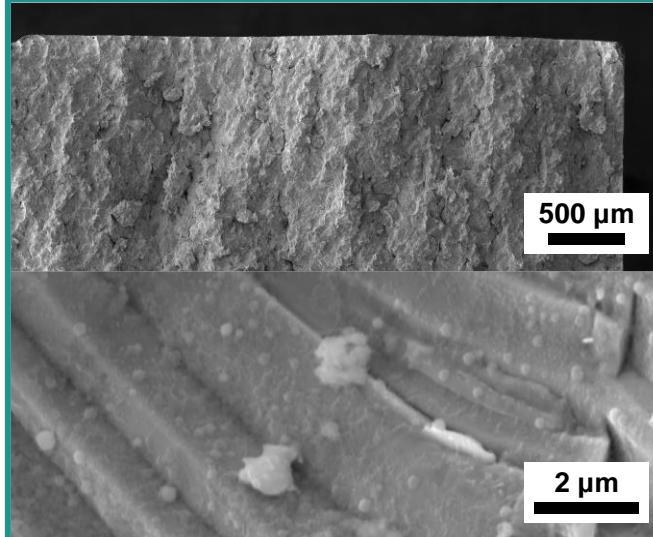
EB-Cast



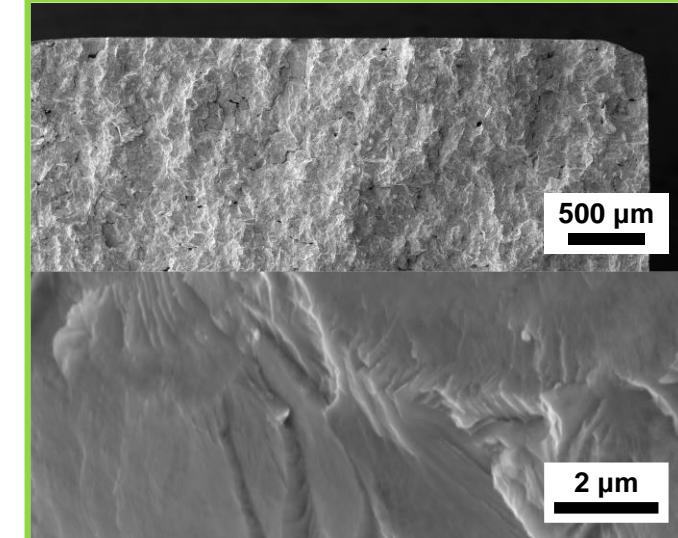
Pure-W



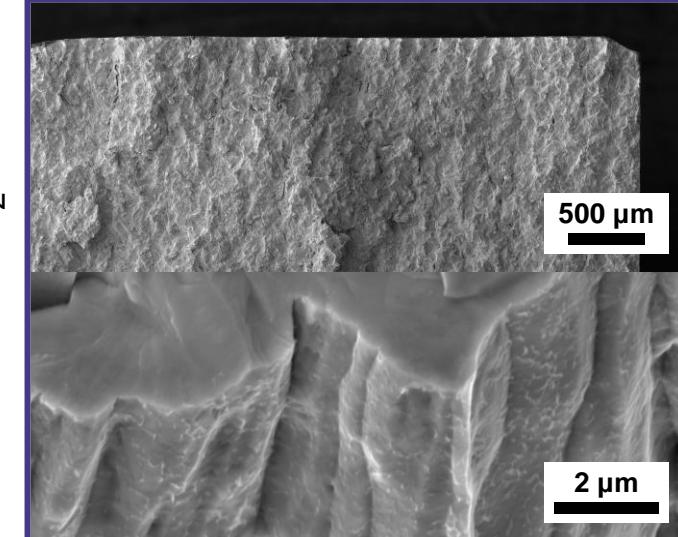
W-HfO₂



W-HfC



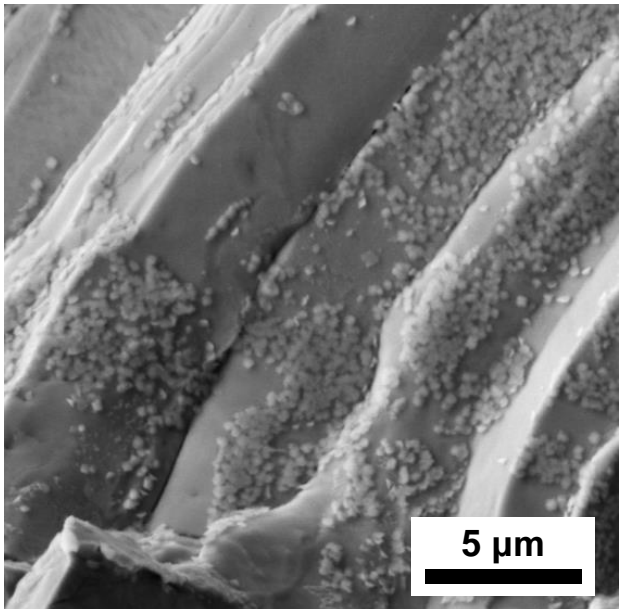
W-ZrH₂



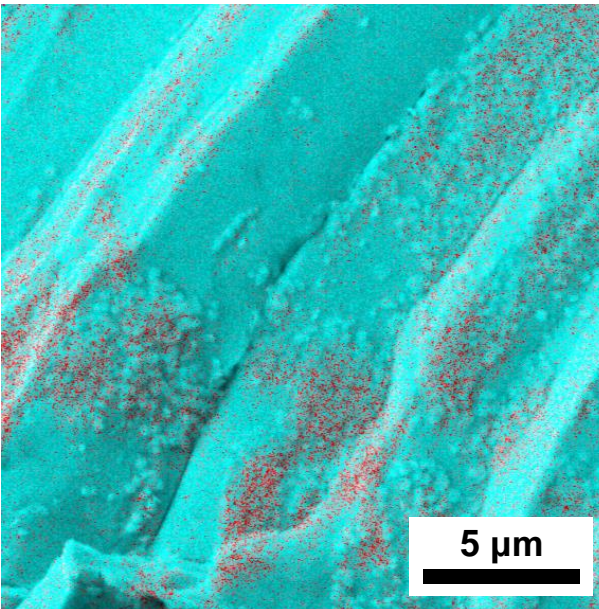
Fractography – EDS of Pure-W



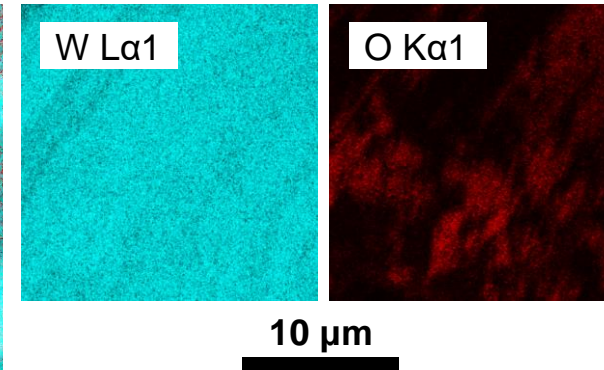
(a) Electron Image



EDS Layered Image

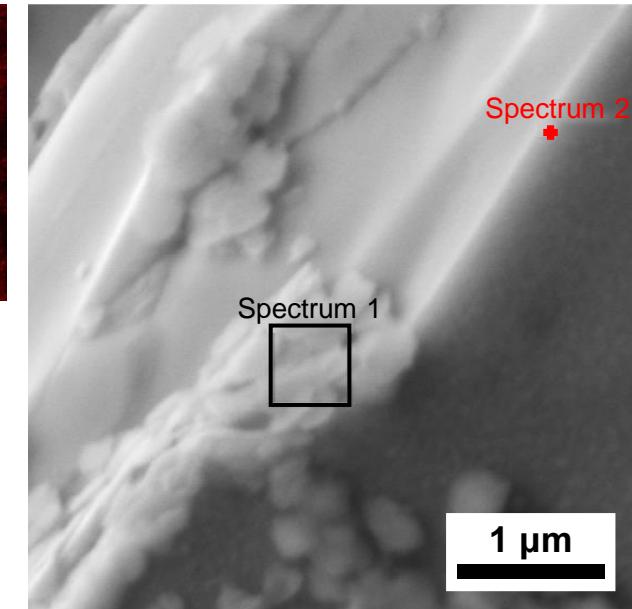


Element Maps



Spectrum Quant.
W 94.2 wt%
O 5.8 wt%

(b) Electron Image

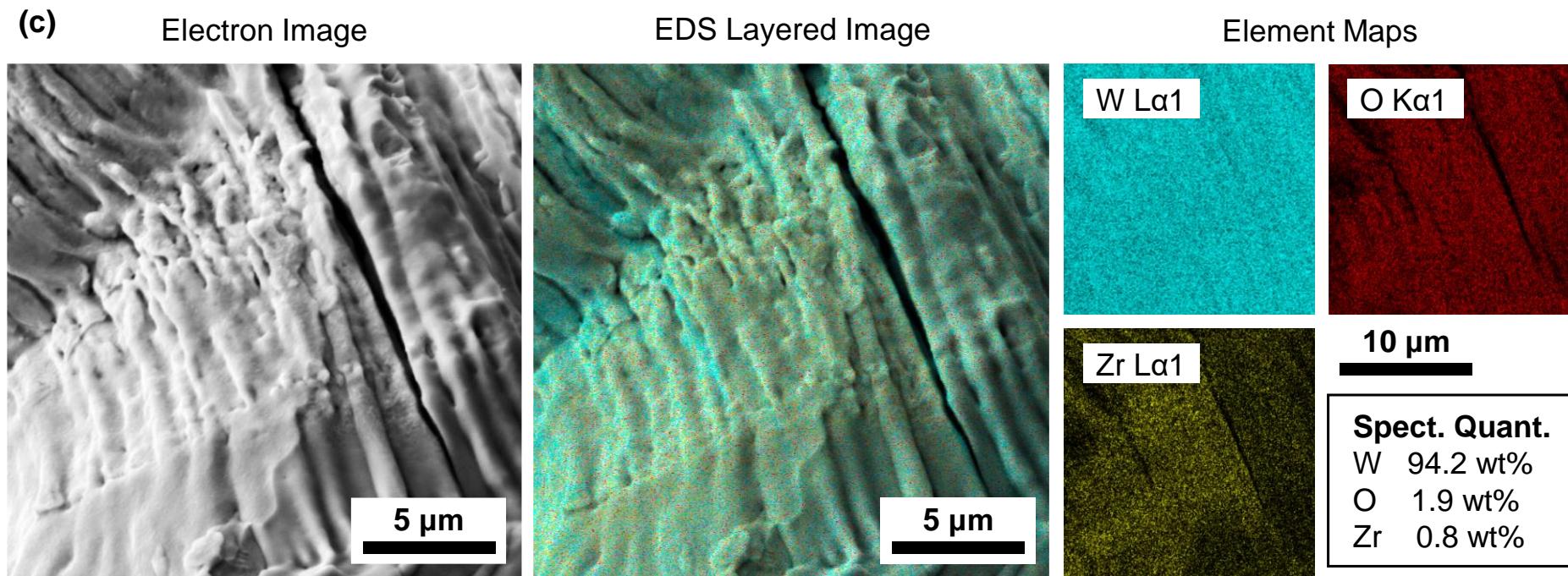


Spectrum 1
W 31.2 at%
O 68.8 at%

Spectrum 2
W 74.5 at%
O 25.5 at%

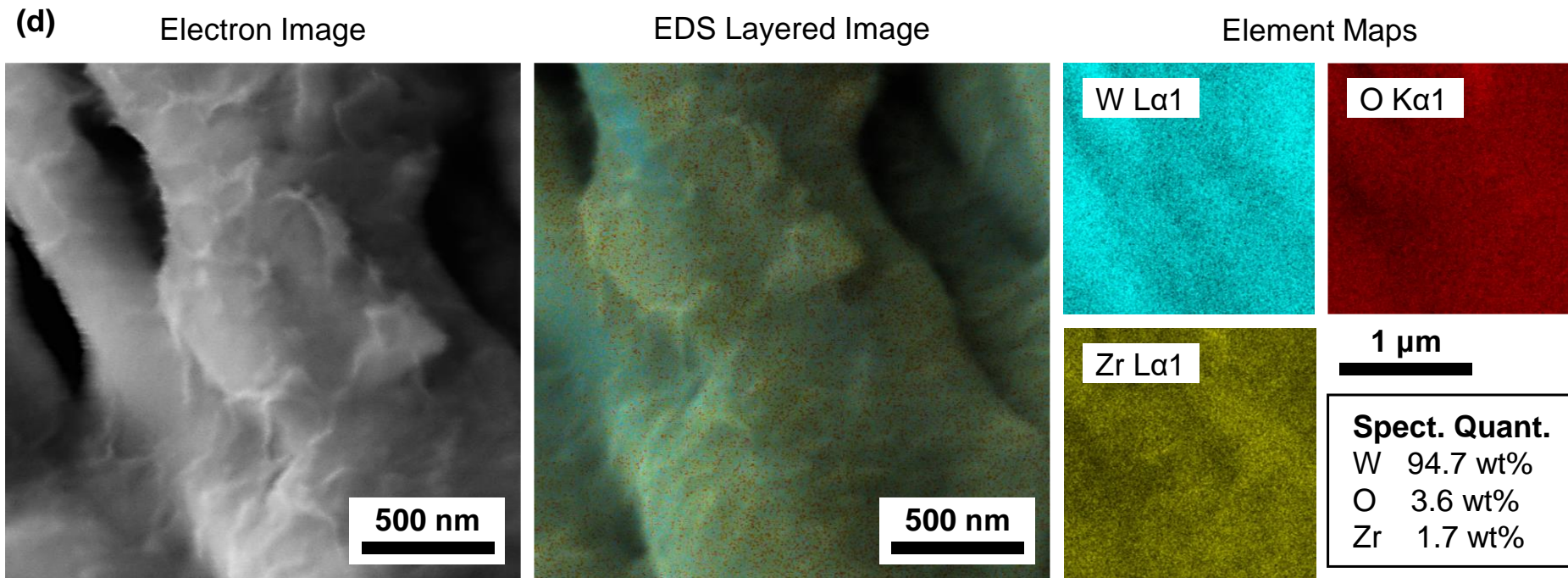
Secondary electron image, EDS layered map, elemental maps, and spectrum quantification of the (a) Pure-W fracture surfaces, alongside EDS verification of tungsten oxide particles on the Pure-W fracture surface (b).

Fractography – EDS of W-ZrH₂



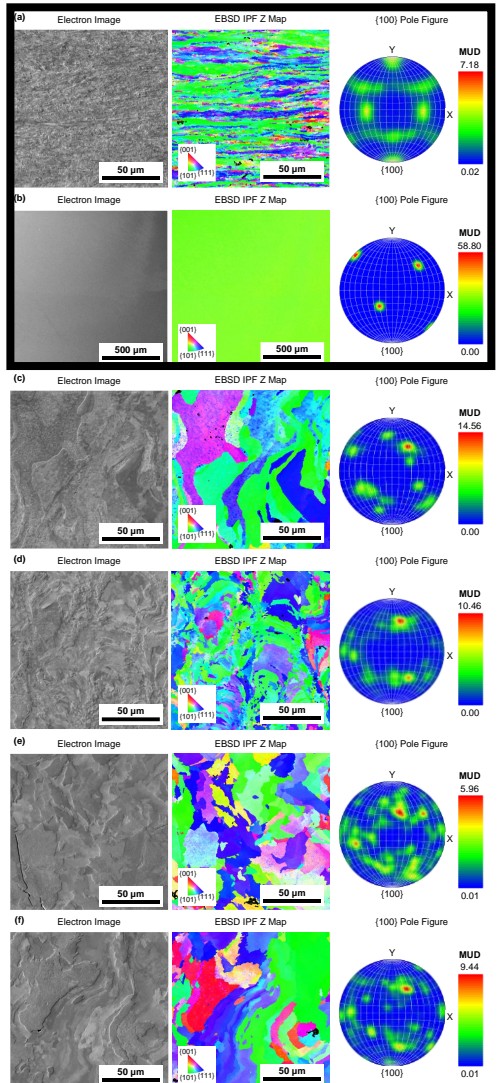
Secondary electron image, EDS layered map, elemental maps, and spectrum quantification of the (c,d) W-1ZrH₂ fracture surfaces

Fractography – EDS of W-ZrH₂ [High Mag]

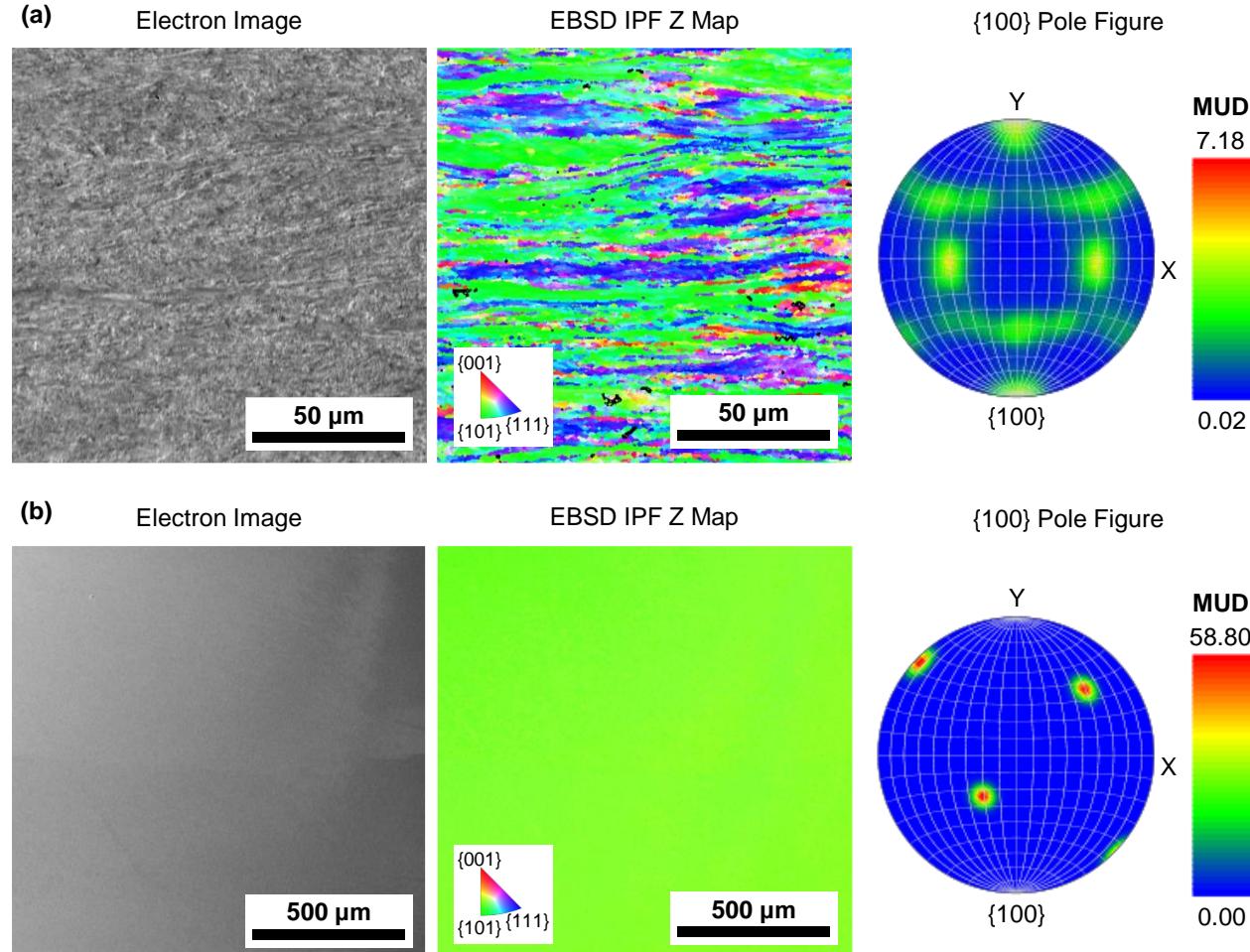


Secondary electron image, EDS layered map, elemental maps, and spectrum quantification of the (c,d) W-1ZrH₂ fracture surfaces

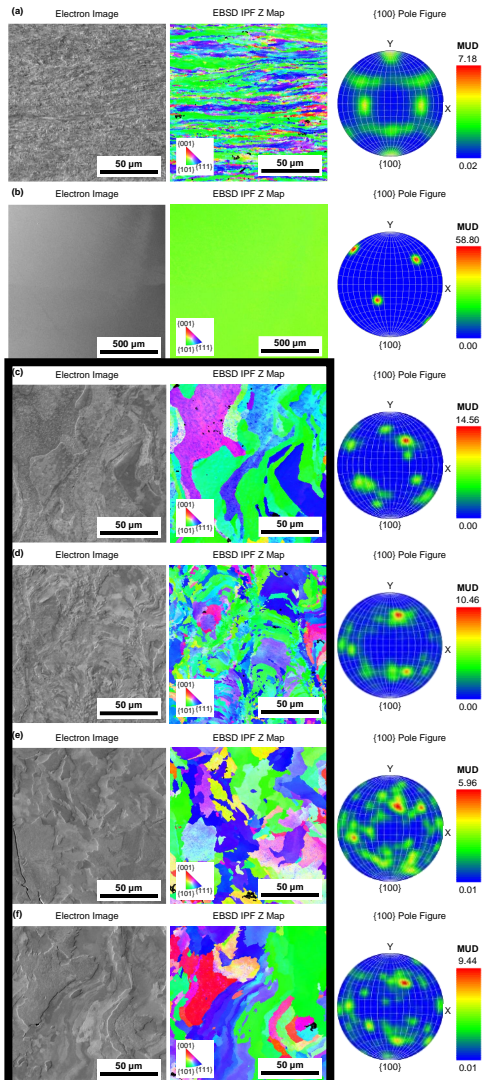
Microstructural Analysis – EBSD



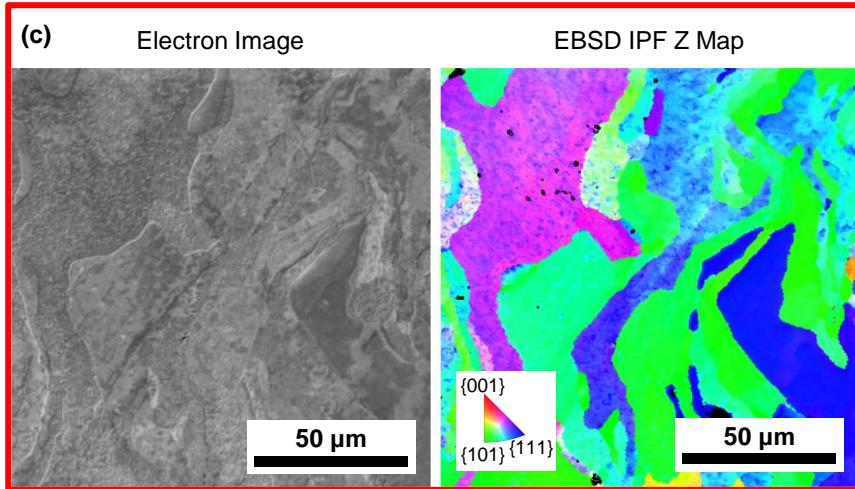
Wrought



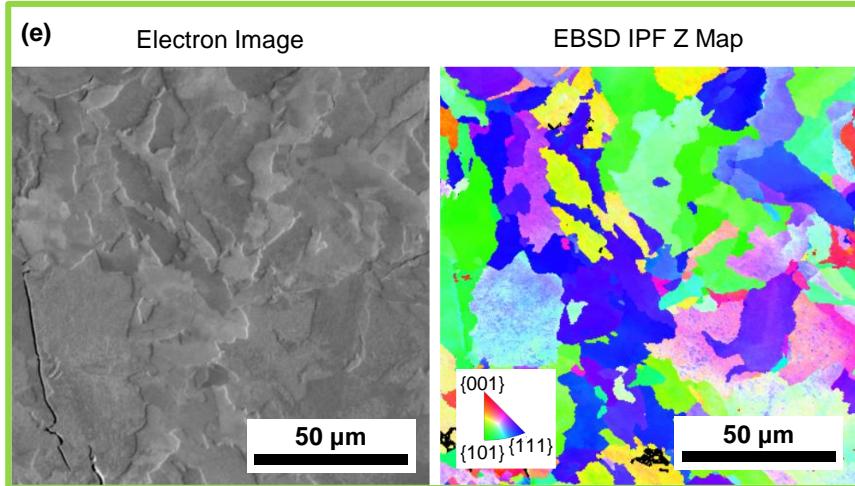
Microstructural Analysis – EBSD



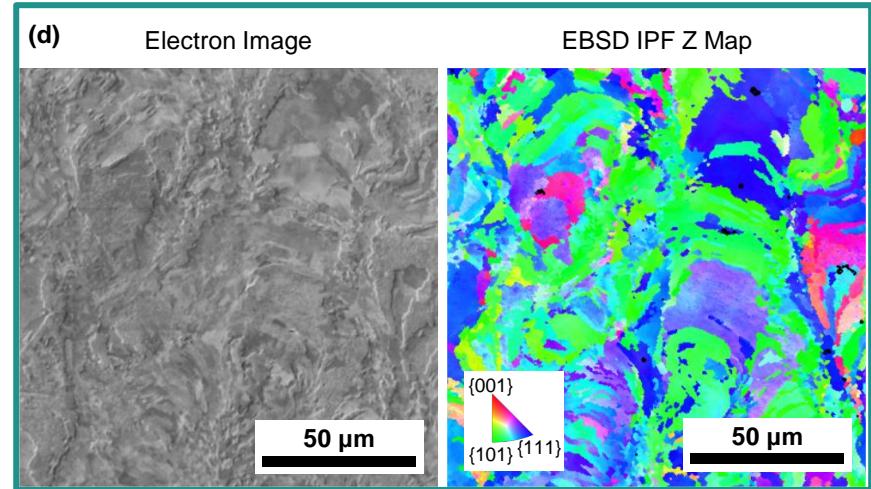
Pure-W



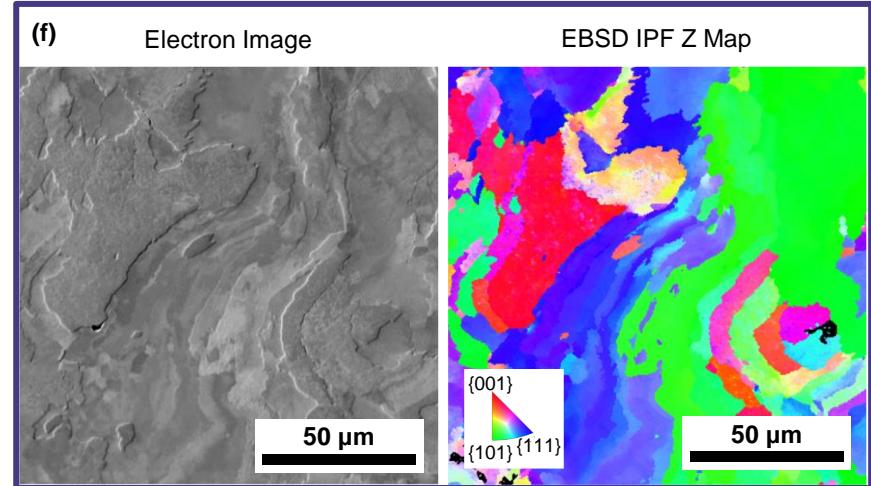
W-HfC



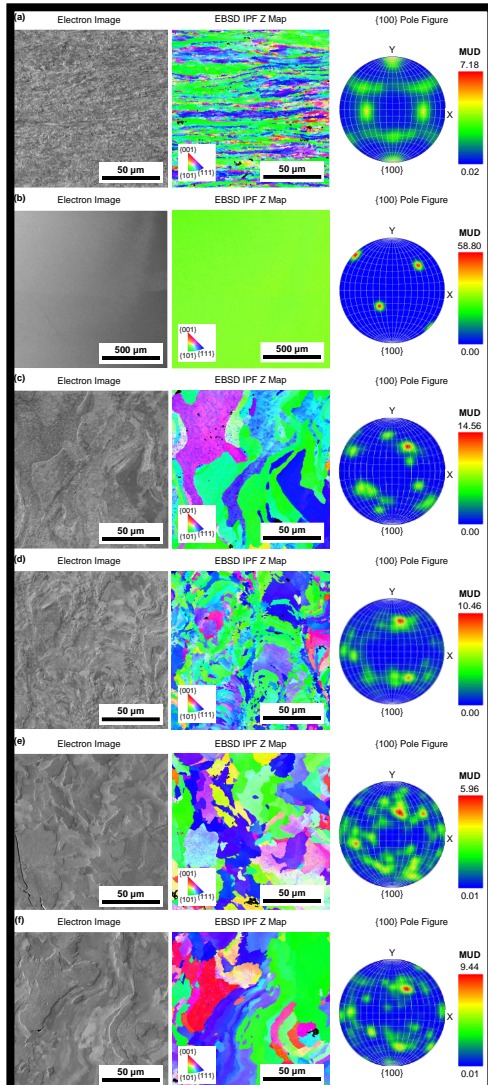
W-HfO₂



W-ZrH₂



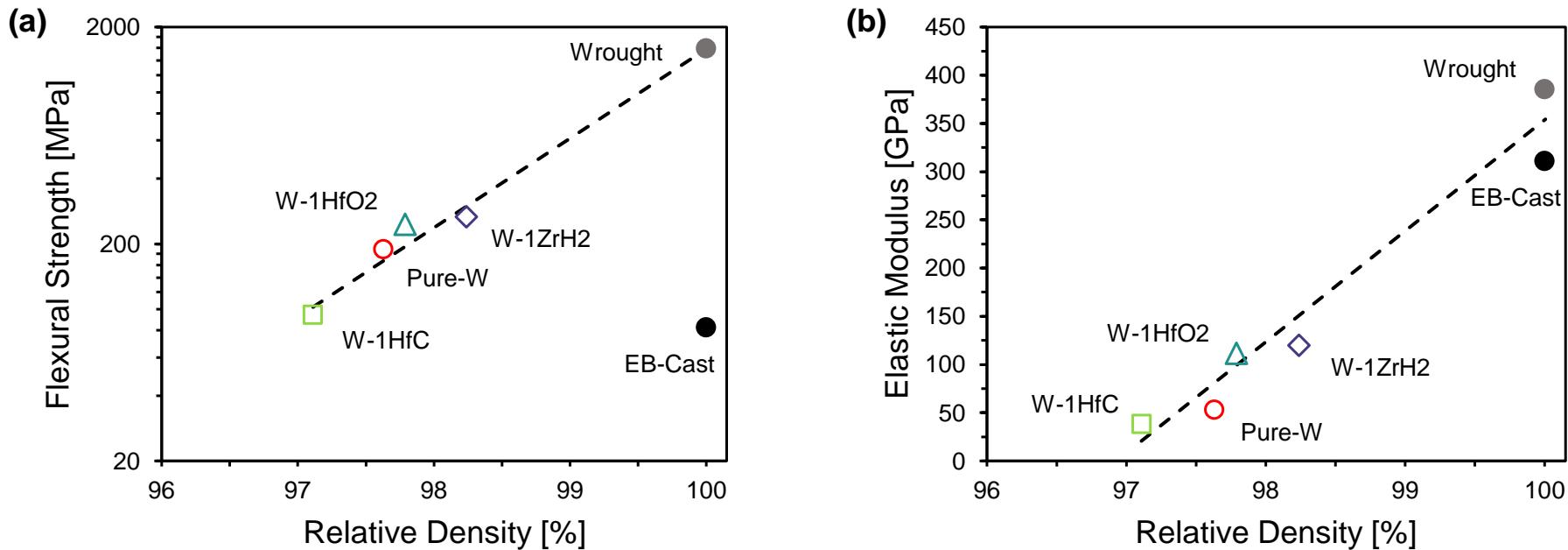
Microstructural Analysis – Grain Statistics vs. Strength



| Material | Flex. Str. [MPa] | Elas. Mod. [GPa] | EBSD Grain Statistics (Average) | | | | |
|---------------------|---------------------|---------------------|---------------------------------|-----------|-----------|---------|---------|
| | | | ECD [μm] | Len. [μm] | Asp. Rat. | GOS [°] | MOS [°] |
| Wrought | 1595.9 | 385.3 | 3.37 | 8.88 | 3.36 | 4.21 | 9.55 |
| EB-Cast | 82.3 | 310.8 | - | - | - | 0.86 | 4.54 |
| Pure-W | 188.6 | 53.0 | 15.73 | 34.34 | 2.95 | 3.06 | 11.83 |
| W-1HfO ₂ | 245.6 | 111.5 | 4.27 | 7.50 | 1.99 | 1.96 | 5.01 |
| W-1HfC | 94.2 | 38.4 | 7.29 | 12.61 | 1.99 | 1.69 | 4.89 |
| W-1ZrH ₂ | 266.5 | 119.8 | 6.91 | 11.92 | 2.03 | 1.72 | 5.57 |

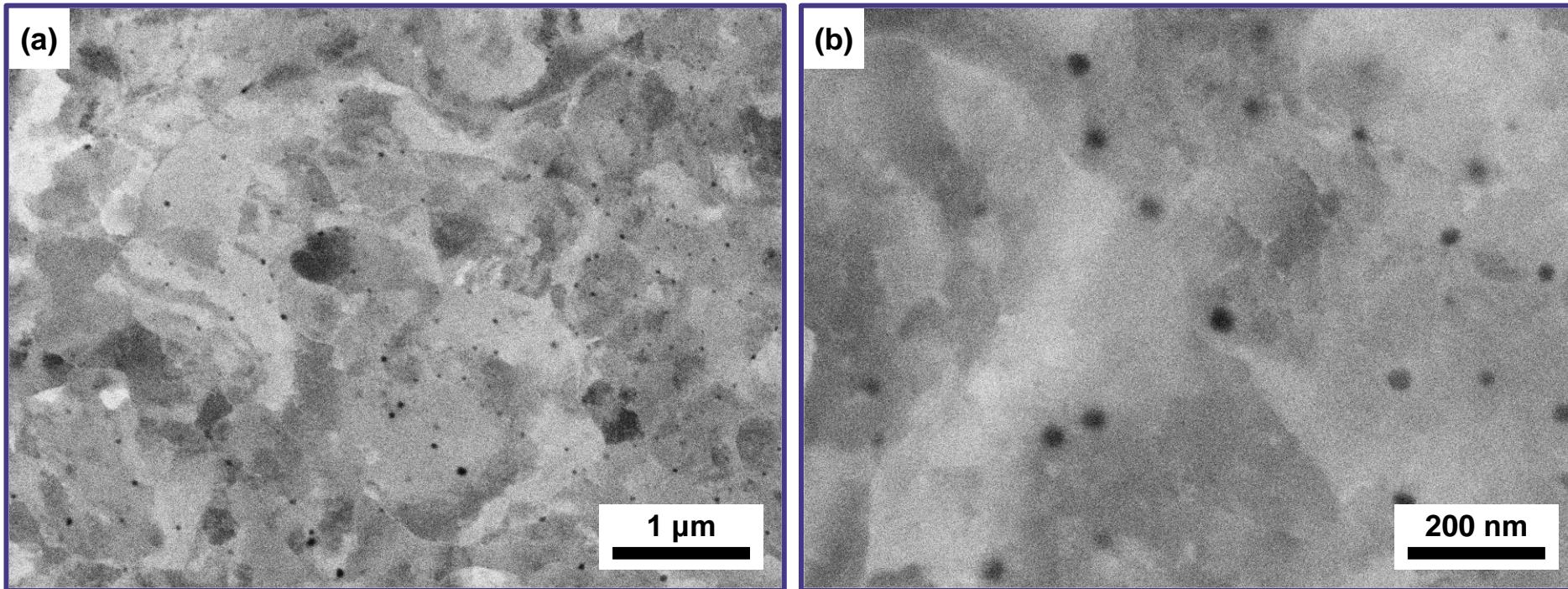
Discussion

- Relative Density is consistent with Flexural Strength



Flexural strength (a) and Elastic modulus (b) vs. relative density for the Wrought, EB-Cast, and L-PBF consolidated materials

Discussion



Low (a) and High (b) magnification backscatter electron images of the W-1ZrH₂ material showing nano-sized particles throughout microstructure



Conclusions

1. Nano-scale HfO_2 achieved the most uniform coating during powder processing
2. The ZrH_2 addition increased L-PBF relative density compared to the **Pure-W** feedstock (97.6 % » 98.2 %)
3. The ZrH_2 and HfO_2 additions increased the L-PBF flexural strength and bending elastic modulus; however, overall performance is far from wrought worked material
4. Both HfC and ZrH_2 additions reduce the detectable oxides on L-PBF fracture surfaces
5. All feedstock modifications reduced the grain ECD, but the HfO_2 addition created finest L-PBF microstructure
6. Material relative density and micro-cracking had the largest influence on mechanical performance

